We are IntechOpen, the world's leading publisher of Open Access books Built by scientists, for scientists

4,800
Open access books available

122,000
International authors and editors

135M
Downloads

Our authors are among the

154
Countries delivered to

TOP 1%
most cited scientists

12.2%
Contributors from top 500 universities

CLARIVATE ANALYTICS BOOK CITATION INDEX INDEXED

WEB OF SCIENCE™

Selection of our books indexed in the Book Citation Index in Web of Science™ Core Collection (BKCI)

Interested in publishing with us?
Contact book.department@intechopen.com

Numbers displayed above are based on latest data collected.
For more information visit www.intechopen.com

16

Corrosion Behavior of Aluminium Metal Matrix Composite

Zaki Ahmad[1], Amir Farzaneh[2] and B. J. Abdul Aleem[1]
[1]*Mechanical Engineering Department, King Fahd University of Petroleum & Minerals, Dhahran,*
[2]*Department of Metals, International Center for Science, High Technology and Environmental Sciences, Kerman,*
[1]*Saudi Arabi*
[2]*Iran*

1. Introduction

Metal matrix composite (MMC) is a material which consists of metal alloys reinforced with continuous, discontinuous fibers, whiskers or particulates, the end properties of which are intermediate between the alloy and reinforcement (Schwartz, 1997). These materials have remained the focus of attention of aerospace, automobile and mineral processing industry because of the several advantages they offer which include high strength to weight ratio, elevated temperature toughness, low density, high stiffness and high strength compared to its monolithic counterpart (the original alloy). The particle reinforced metal matrix composites (PRMMC) satisfy many requirements for performance driven applications in aerospace, automobile and electrical industry. The particle reinforced composites can be tailored and engineered with specific required properties for specific application. The commonly used reinforcing materials are silicon carbide, aluminium oxide and graphite in the form of particles and whiskers. Nominal compositions of some well known alloys which are reinforced with whiskers, fibers or particulate is shown table 1. Figure 1 shows that microhardness increases with an increase in filler content of the composites.

	Si	Fe	Cu	Mn	Mg	Cr	Zn	Ti	Al
Al 6061	0.62	0.23	0.22	0.03	0.84	0.22	0.10	0.1	Bal
Al 7075	0.40	0.50	0.60	0.30	2.5	0.15	5.5	0.2	Bal
Al 6013	0.6	0.50	1.1	0.2	0.8	0.1	0.25	01	Bal

Table 1. Nominal composition of some well known alloys reinforced with whiskers and particles

MMC can be continuous or discontinuous. Discontinuous MMC can be isotropic and can be worked with standard metal working techniques such as extrusion, forging or rolling.

Continuous reinforcement uses monofilament fibers, wires or fibers such can carbon fibers. The reinforcement materials commonly used are graphite SiO_2, SiC, TiC, Al_2O_3 and glasses.

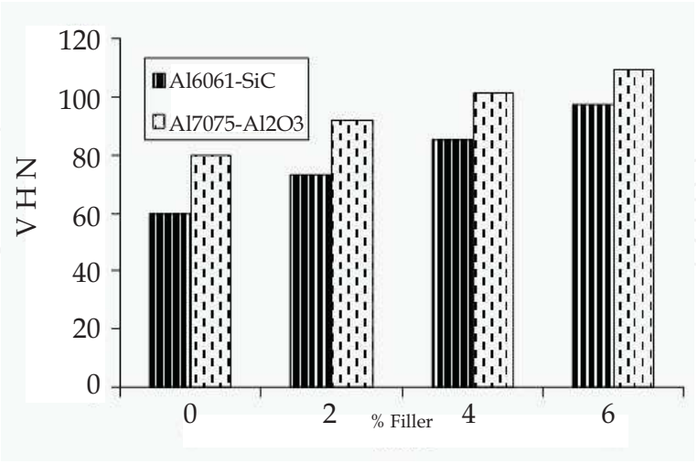

Fig. 1. Microhardness of Al6061-SiC and Al7075-Al2O3 composites (Vaeeresh et al., 2010)

2. Mechanical and physical properties

Metal matrix composites have been shown to exhibit significant improvements in certain physical and mechanical properties over their monolithic metallic counterpart, However, the mechanical properties are strongly dependent on micro structural parameters, in particular, size, shapes volume fraction and orientation of the particles and the composition of matrix.

Parameters	Al 6061	Al 7075	SiC	Al2O3
Flastic Modulus	70 – 80	70 – 80	410	300
Density	2.7	2.81	3.1	3.69
Poisson's Ratio	0.33	0.33	0.14	0.21
Hardness (HB – 500)	30	60	28 W	1175
Tensile Strength(MPA)	115	220	3900	2100

Table 2. Properties of Al 6061 and Al 7075 with and without reinforcement

It is a general observation that the Vickers microhardness observed is greater than the matrix alloy. This is a exemplified by composites, 6061/SiC(p), 6013 SiC(p) and 7075/Al2O3(p) Figure 1 shows the effect of Vol.% of particulates (SiC) on the modulus of elasticity of Al 6061 / SiC, and Al 7075/ Al2O3 composites (Vaeeresh et al., 2010).

The development of metal matrix composites has been a major breakthrough in the last twenty years. The quantum leap in recent years has established their potential for weight critical application in engineering components and structures in aerospace.

It is shown that the tensile strength is increased with increasing volume fraction of SiC particulates. This applies to all metal matrix composites including discontinuously reinforce composite reinforced with SiC particulates or whiskers Figure 2 and 3. The effect of strength may be attributed to the generation of dislocations on cooling of the metal matrix

composites. Such dislocations have been observes by TEM. A high dislocation density was observed on Al 6013/SiC (p) interface.
In a TEM experiment, the generation of dislocations started only at 500 K (Vogelsang et al. 1986). It has also been suggested that dislocation were generated in Al – 6061/ 20 SiC MMC below 573 K.

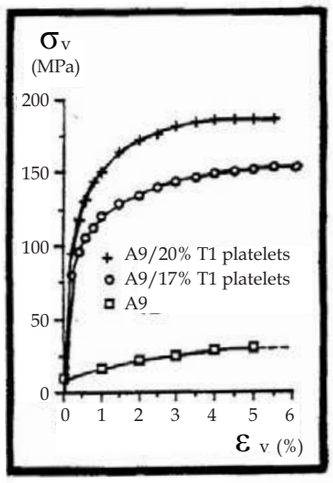

Fig. 2. Effect of the size of the platelets (Massardier et al., 1993)

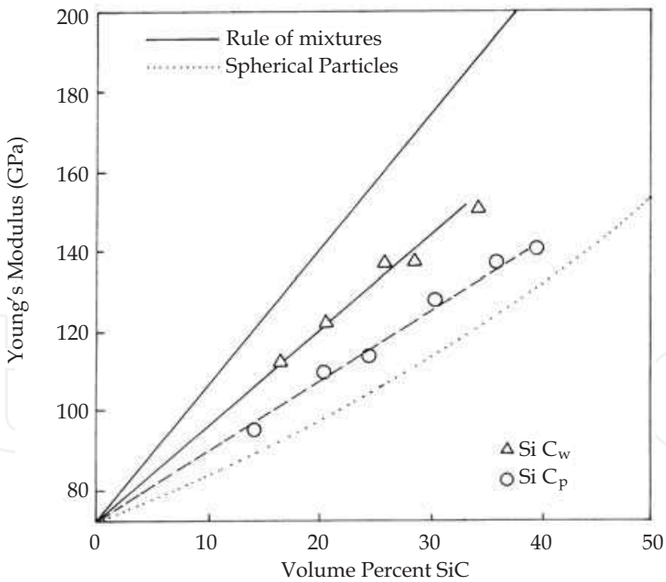

Fig. 3. Young's modulus vs volume percent of SiCw, SiCp and reinforcement (Zaki, 2001)

The elongation (%) of the MMC decreased with increased particulate contents as shown by Al 6061 / 20 SiC (p) – The mechanism of fracture toughness is not fully understood. The presences of large clusters of particles promote crack propagation whereas their uniform distribution retards crack propagation. The fracture toughness values of selected alloys are given in Table 3.

Alloy Designation	Toughness Value
Al2009/ SiC/15(%) W (T 8)	51 mpa √m
Al6061 – 40% SiC(p)	122 mpa √m
Al6013-29SIC(p)	19.5 KSi√2

Table 3. Fracture toughness of selected MMCS

The strains to failure (%) for different Al_2O_3 reinforcement are shown in Table 4 Strain to failure decreases with increase of volume fraction of reinforcement.

Vf %	Percent strain to failure
	(Ef)mm/mn*100
Al 6061	29.26
Al 6061 / 10 vol.% Al2O3	4.72
Al 6061 / 20 vol.% Al2O3	2.29
Al 6061 / 30 vol% Al2O3	1.42

Table 4. Strain to failure of Alloy Al 6061 with increasing volume fractions (Dehlan and Syed, 2006)

Al MMC are finding increasing applications as rotor material in automotive brake systems (Shorowords et al., 2004). Effect of Studies on the effect of sliding velocity on wear friction and tribochemistry of MMC reinforced with 13% SiC or B4C have shown that sliding velocity leads to lower wear rates and lowers friction coefficient for both MMCs.. Studies on interaction between MMC and phenolic brake pads showed that the transfer layer consisting of phenolic pad material acted as a protective layer and reduced wear rates and coefficient of friction. Honda has used aluminum metal matrix cylinder liners in some of their engines including B2lAl and H23A, F20 C and F22C.

The effect of cutting speed on tool wear has been investigated. The cutting tool wear increased with increased reinforcement ratios. At constant speed and feed rate, the lowest wear rate has been found in 5 Wt % SiC (p) and the highest wear with 15 Wt % SiC_p increased cutting speed increased the tool wear rate.

From the above description, it may be concluded that the development of MMC has been a big breakthrough in search for stiff high strength materials for aerospace and automotive industry particularly. Whereas the mechanical properties of MMC have remained the focus of attention, the work on corrosion behavior of MMC did not proceed hand in hand with the mechanical and tribological properties. The work on corrosion was undertaken the last decade and a considerable progress has been made in the understanding of corrosion behaviour of metal matrix composites in recent years.

3. Corrosion behavior of Aluminum metal matrix composites

The corrosion behaviour of alloys in sea water 3.5 Wt % NaCl represents an adequate measure of its corrosion resistance. Important results of corrosion studies undertaken in the last decade would be discussed under the following categories.

a. Immersion and long term exposure tests in sea water or 3.5 wt % NaCl.
b. Localized corrosion studies
c. Flow induced corrosion and Erosion corrosion
d. Corrosion inhibition
e. Corrosion mechanism

3.1 Immersion & long term exposure studies

The above studies were conducted in accordance with ASTM designation G 31 – 72 (ASTM, 2004). The results of studies on Al6092 – T6, Al/*B*4C/20P, Al 6092 – T6 /2oSiC(p), and 6092 – T6 20vol%Al2O3 and monolithic 6061-T6 Al, immersed for 90 days in air exposed 0.5 Na_2SO_4 solution, 3.5 wt% NaCl, ASTM sea water and real sea water were recently described (Hongho et al. 2009). In alloy 6092 – T6 Al/B 4C/20P MMC specimen in ASTM Sea water bubbles were observed. The current over most of the area was found to be anodic. The solution at the anode site was found to be acidic (PH 6.4). Corrosion products were formed as observe after monitoring for three days and the area became more alkaline (PH 8.4). A similar phenomena occurred with alloy 6092 reinforced with 20 Vol. % SiC (p) and gradually the alkalinity increased because of its change of area from and anodic to cathodic. The corrosion rates of MMCS in sea water and ASTM sea water were lower than those in 0.5 M Na_2SO_4 and 3.5 wt % NaCl. The rates of monolithic 6061 – T6 Al in both real and ASTM sea water were significantly lower than those in 3.5 wt % NaCl. The surface morphology after the test showed similar general features, one major feature of the surface morphology was the presence of intermetallic precipitates on the surface. The EDS studies suggested these precipitates to contain Al, Mg, O, and C. Mg and HCO_3 irons as the main species corrosion products.

The formation of precipitates is a greater concern in MMC, as localised corrosion is controlled by the formation of such precipitates. The role of precipitates would be discussed in the relevant section of the paper. In general the corrosion rate of Al MMC decreased with time due to the formation of precipitates.

3.2 Localled corrosion of ALMMC's

If is generally accepted that MMC are in general more prone to corrosion than their monolithic counterparts (Berkely et al., 1998; Turnbull and Corros, 1992; Trzskoma, 1991). Conflicting views have been presented on the causes of the localised corrosion. The results of the studies showed that galvanic corrosion between the matrix and the reinforcement occurs. However, this is related to the machining conditions. Three different machining process; Wielding Electrical Discharge Machine (WEDM), Cemented Carbide Turning and Single Point Diamond Turning were employed for investigation. The test results for different process are shown in Table 5 (Yue et al., 2002).

	E_{Corr} (mV)	E_{pitl} (mV)	$E_{Pil} - E_{corr}$ (mV)	I_{Corr} (Am^{-l})
WED	–761.4	– 633 v	128.4	3.80 TE – 4
Carbide Turning	– 673.6	– 655	186	3.194 E – 2
Diamond Turning	– 928.3	– 655	288.3	1.052 E – 3

Table 5. Electrochemical parameters for different machining conditions (Yue et al., 2002)

The electrical discharge machining showed the highest value of pitting potential. The resolidified layer did not show any extensive pitting. The results show that surface conditions have a major effect on pitting potential and the resistance to pitting may be shown by E_{pit} - $E_{Corrosion}$. The difference above is not sufficient to predict corrosion susceptibility. It may be observed that silicon carbide is an insulator and there is hardly any possibility of cathodic reaction occurring on the surface of particles. The theory that Al/SiC is sensitive to corrosion because of micro galvanic coupling applies to some intermetallic compounds, cathodic to the matrix such as $CuAl_2$ which is formed. So far there is no general agreement on the role of SiC particulates on the mechanism of localized corrosion. The electrochemical behaviour of Al2024/AlSiC has been also investigated by scanning micro reference electrode imaging system (Feng et al., 1981; Isacs & Vyas, 1981). The results of investigations on Al2024/Al SiC (A) are given in Table 6.

Volume Fraction	$E_{pitting}$			$E_{protection}$			$E_{corrosion}$	
	0.01 m NaCl	6.1 m NaCl	0.5 m NaCl	0.01 m NaCl	0.1 m NaCl	0.5 m NaCl	0.5 NaCl	0.1 NaCl
0	– 430	– 497	– 565	– 653	– 620	– 612	– 612	– 574
5	– 460	– 528	– 597	– 750	– 700	– 670	– 670	– 610
10	– 485	– 555	– 625	– 740	– 765115(T)	– 720	– 725	– 688
15	– 538	– 632	– 662	– 700	– 720	– 720	– 750	– 671
20	– 550	– 650	– 692	– 670	– 670	– 775	– 775	– 671

Table 6. Summary of electrochemical data (Feng et al., 1981; Isacs & Vyas, 1981)

It was observe that pitting potential E_p decreased as the volume fraction of SiC particulate reinforcement increased. The relation between the volume fraction and $E_{Protection}$ It was clearly observed that the pitting attack occurred at SiC/Al interface which contained intermetallic Cu and Al precipitates. The presence of Mg, Cu, and Fe compounds in Al6013/20% Vol. of SiC has been confirmed also in another work in recent years (Zaki et al., 2000). The interfacial regions may act as active centers for localized corrosion on immersion in sodium chloride solution. The EDS spectrum of Al_2Cu is shown in Figure 4. The pits on Al 2024/SiC interface are shown in Figure 5. In Al 2024/SiC MMC, Mg may segregate in addition to the precipitates of Al_2Cu Mg and Al_2Cu. The segregated magnesium may form active galvanic couple with Al matrix (Jamaludin et al., 2008). There is also the possibility of the intermetallic precipitates to act as local anodes or cathodes because of the difference between the open circuit potentials of these intermetallic with Al matrix. As seen above the role of the precipitates and inclusion is not clearly understood. However, the evidence of localized corrosion of Al MMC suggests, that the Al/SiC interface in active and responsible for localized corrosion. This is also confirmed by studies on (Al 2009/SiC W) (W = whisker). In the rolled material extensive pitting occurred, and on removing the corrosion products it was observed that the pits contained particles $CuAl_2$ (Rohatgi, 2003). On heat treatment the amount of $CuAl_2$ particles was significantly reduced (Rohatgi, 2003) and the rate of corrosion also diminished which suggested that the heat treatment diminished Mg, Fe and $CuAl_2$ precipitates Figure 6 shows the effect of heat treatment on the corrosion behaviour of T6 and as rolled Al 2009/Sic (w) composite. The corroded surface of as rolled specimens is shown in Figure 6.

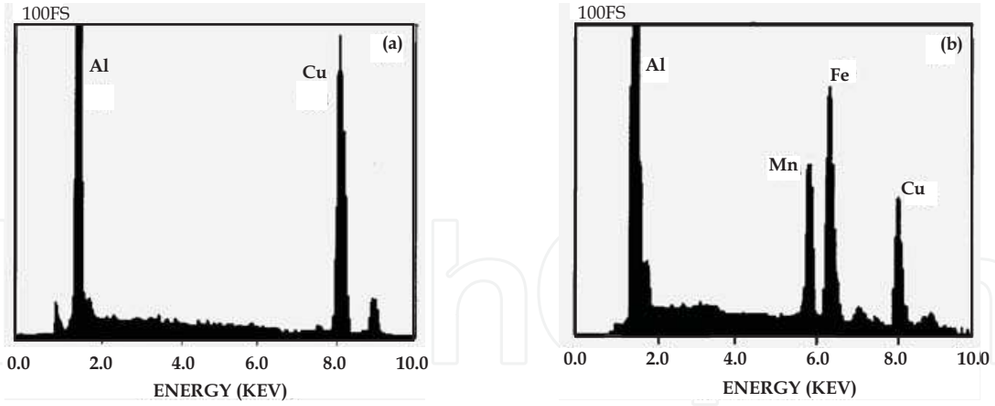

Fig. 4. EDS spectrums of (a) Al2Cu and (b) (CuFeMn) Al6 inclusions (Feng et al., 1998)

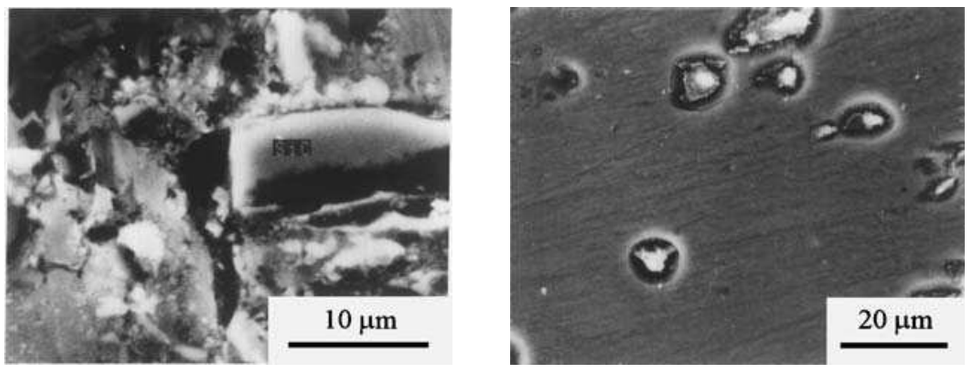

Fig. 5. Scanning electron micrographs of pits on interfaces of (a) SiCp-2024 Al matrix, and (b) inclusions-2024 Al matrix (Feng et al., 1998)

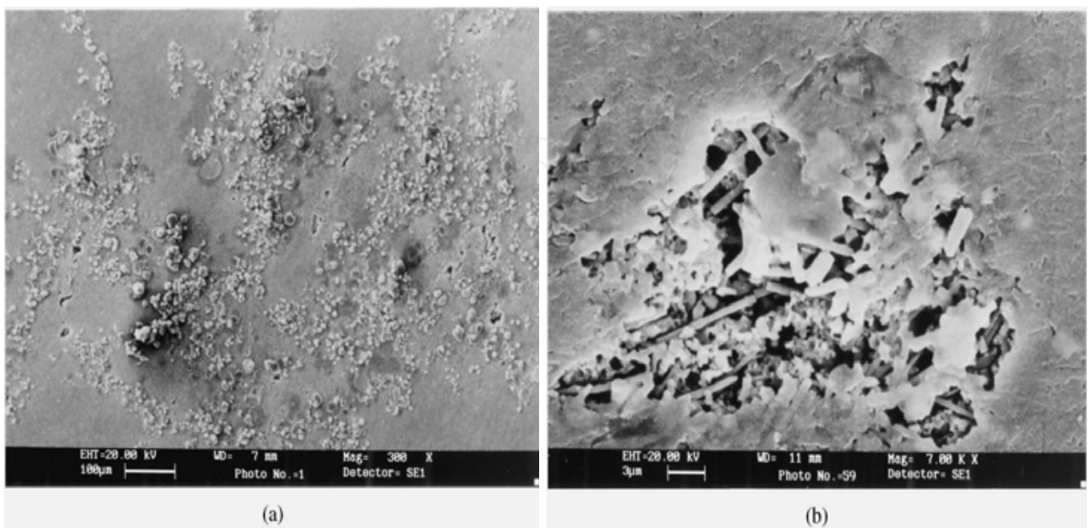

Fig. 6. Corroded surface of the as-rolled specimen after the polarization test (a), (b) showing pit morphology (Yue et al., 2000)

3.3 Flow induced corrosion and Erosion corrosion

The resistance of metallic equipment and structures to the impact of flow induced corrosion is extremely important as it affects their operational life and integrity of equipment. Whereas the effect of velocity on the erosion/corrosion of steel copper, and aluminium alloys are widely reported in literature the information on the metal matrix composite is scanty (Rohatgi, 2004; Griffen &Turnbull, 1994; Lin et al., 1992; Mansfield & Jeanjagnet, 1984; Chen & Mansfeild, 1997; Hihara, 2010; Colman et al., 2011). Studies on Al 6013–20 SiC were conducted in a customized recirculation loop as shown in Figure 7. It consisted of entry valves, a manometer, a centrifugal water pumps, a flow meter and several specimen holders to accommodate flat specimens. Each specimen holders contained four specimens which were housed in an outside container. The velocity was varied by varying the chamber of the specimen holders. Three tempers of Al6013-20 SiC (p) were investigated in the loop. In which a solution of 3.5wt%% NaCl was flowing at velocities ranges from 1-4 ms^{-1}.

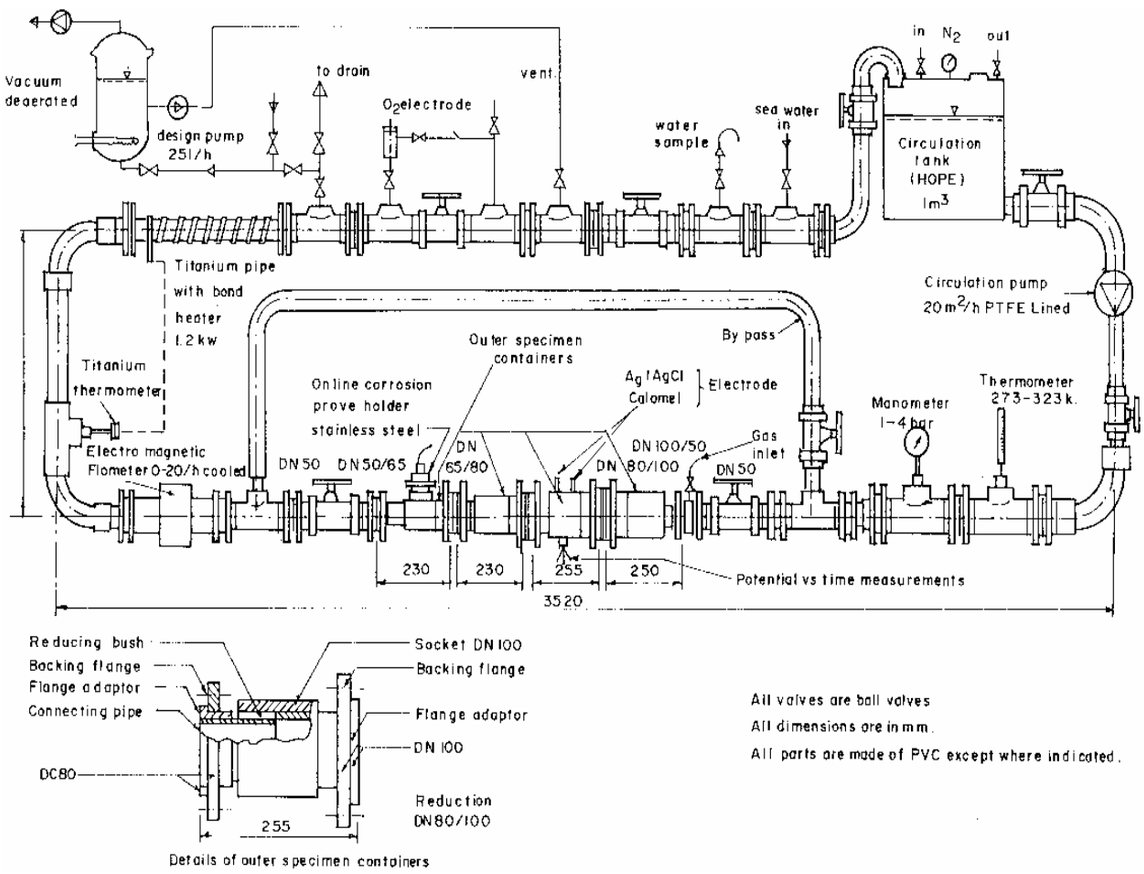

Fig. 7. Schematic diagram of PVC recirculating loop (Zaki, 2001)

After exposure of 100 hours it was shown that temper (0) annealed, and temper F, as fabricated, showed a lower resistance to corrosion in 3.5 wt% NaCl with and without polystyrene suspended particles. Upon increasing the temperature form 30 to 50 and 90 C, the erosion corrosion rate increased as shown in Table 7 and 8 (Zaki, 2007).

	Corrosion Rate(In 3 weight% NaCl + Vol% Polystyrene(mpy)		
Velocity	Temper(0)	Temper (F)	Temper T4
1.0	11.8	9.9	9.6
2.7	12.6	10.8	10.1
3.8	12.9	11.3	11.4

Table 7. Variation of Erosion-Corrosion Rate with Velocity in 3.5wt%% NaCl + 2%Vol Polystyrene (Zaki, 2007)

		Erosion Corrosion Rate(mpy)		
Temperature (^oC)	Velocity	Temper(O)	Temper(F)	Temper(T4)
50	1.0	12.1	10.3	9.9
	1.9	3.6	11.2	10.1
	2.7	14.2	12.1	11.4
	3.8	14.9	13.6	10.3
75	1.0	11.9	11.9	117
	1.9	15.5	15.5	161
	2.7	172	17.2	148
	3.8	19.6	19.6	159
90	1.0	13.3	13.3	12.3
	1.9	13.1	15.1	13.6
	2.7	17.8	17.8	163
	3.8	19.7	19.7	17.6

Table 8. The effect of temperature on the erosion – corrosion behavior of Al 6013 – 2051 C (p) in 3.5 wt % NaCl + 2%Vol Polystyrene (Zaki, 2007)

The erosion-corrosion rate increased, linearly with velocity in the presence of SiC particles. It was also found that Temper (T4) of the alloy showed the best resistance to corrosion. The rate of erosion corrosion varied also with temperature. The best resistance offered by T4 may be attributed to the homogenization of the surface structure, less clustering of SiC particles, a uniform distribution of secondary intermetallic phases such as $CuAl_2$ and minimization of micro-crevices (Zaki, 2000). The localized attack was confined to Al 6013/20 SiC (p) interface. A large number of secondary phase particles were observed. After studies showed the presence of Cu 3.55 %, Fe 1.77 %, Mg 1.71 %, and some Cl (0.32%) a high dislocation density was observed at the interface Figure 8 (Zaki, 2000). The formation of coherent films was made more difficult by the protrusion of the particles. This factor adds significantly the erosion –corrosion caused by polystyrene particles. The surface is subjected to a cycle of destruction and reformation of a protective film as a result of impact of polystyrene particles. The corrosion product which accumulates at the interface may act as cathode and increase the cathode / anode area ratio causing an overall increase in the rate of corrosion.
Alloy Al 6013 / 20 SiC (p) in temper T4 offered of temper T4 offered a good resistance to erosion–corrosion. It can be used in water containing Silica or other particulate matter without undertaking any major risk. Al 6013 reinforced with 20 Vol. % SiC (p) was designed to have improved mechanical properties over those of AAl11 6061/SiC (p). The corrosion resistance of al 6013 /20 Sic (p) was determined in fog testing cabinet (Zaki, 2000). A

schematic of salt spray chamber is given in Figure 9. The cabinet comprised of a basic chamber level matic test reservoir (1.0 gal salt solution), reservoir (3.0 gal), bubble tank, twin optic fog assembly, and accessories such as a lower assembly bubble tank heater, control valves, and cabinet heaters. The cross section of the assembly is shown in Figure 10. The results obtained for O, F, and T4 Tempers of the alloy composite in the fog cabinet are shown in Table 9.

Fig. 8. TEM micrograph of Al 6013/SiC interface showing dislocation generations

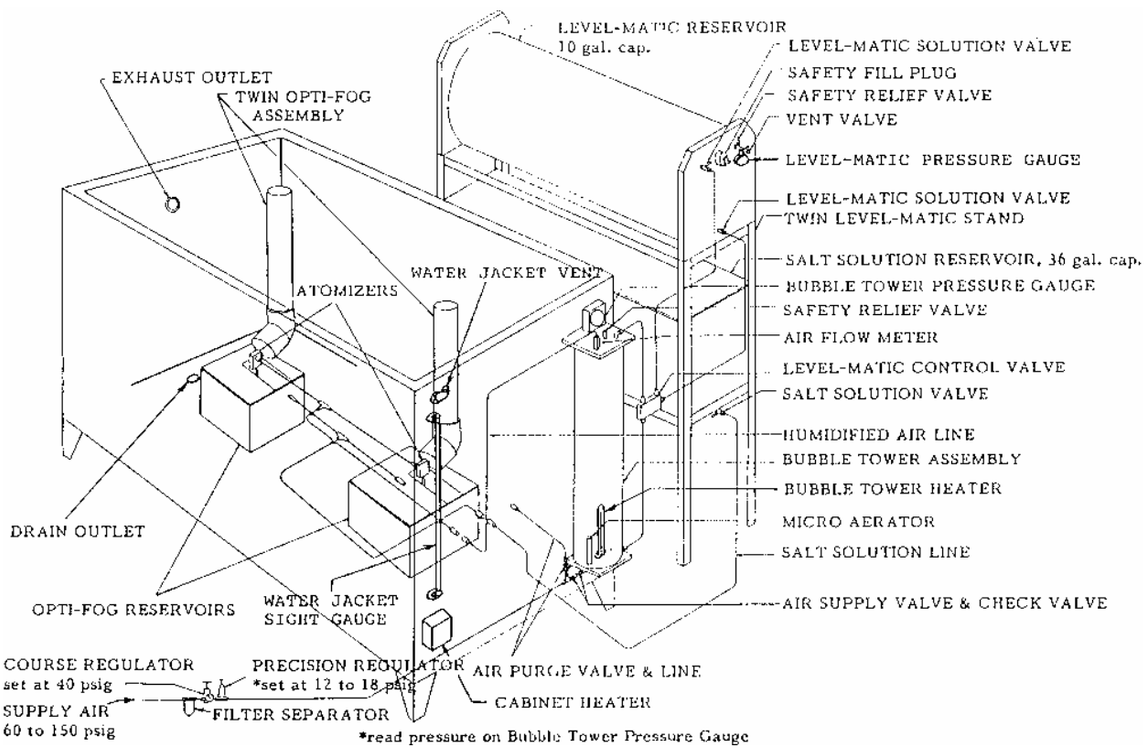

Fig. 9. A schematic of salt spray chamber

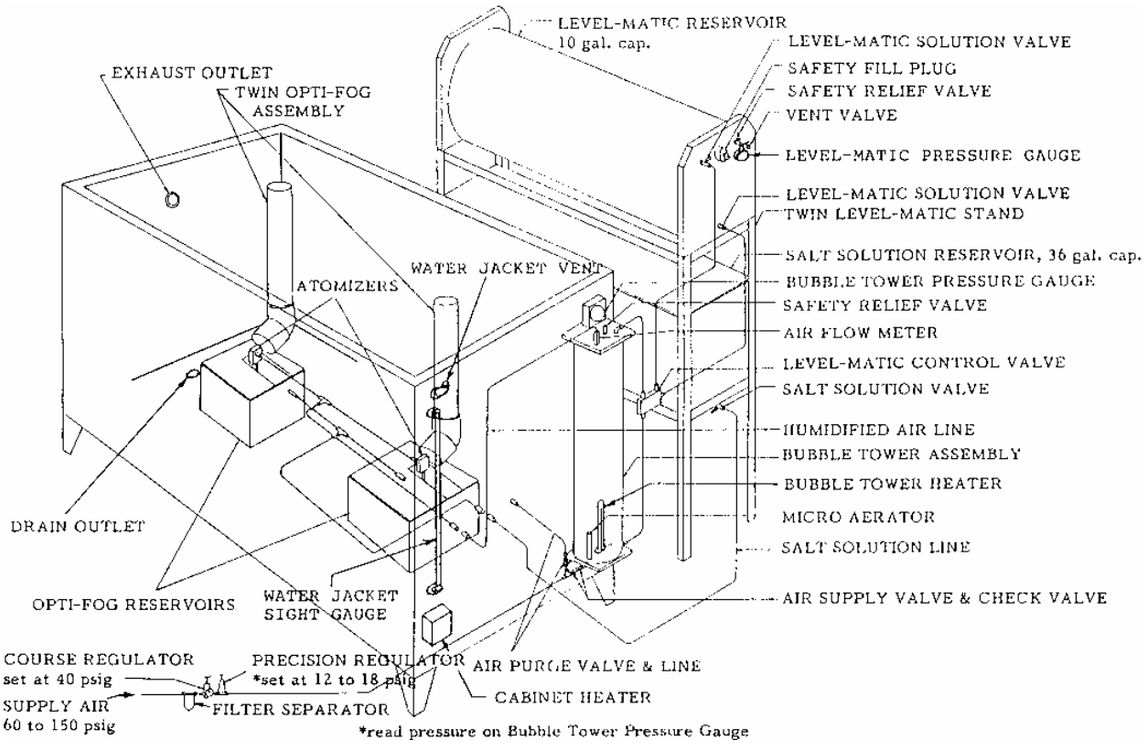

Fig. 10. Cross section of singleton salt fog corrosion test cabinet

Time	Temper-0	Temper-F	Temper-T4
200	10.23 V (19.8)	8.42 (15.78)	7.12 (13.35)
400	9.11 (17.8)	7.78 (14.58)	6.18 (11.09)
600	6.38 (11.96)	6.06 (9.49)	4.38 (8.21)
800	21.92 (9.23)	3.98 (7.46)	2.82 (5.28)
1000	4.66 (8.74)	3.76 (7.05)	2.63 (4.53)
1200	4.27 (8.01)	3.68 (6.90)	2.50 (4.83)

Table 9. Corrosion rates of Al6013/20SiC(p) in Salt Spray Chamber

A decrease in corrosion rate with increased exposure period was observed for all three tempers. The MMC temper T4 showed the highest resistance to pitting. The surface of the composite was often covered with a gelatinous product of aluminum hydroxide $Al(OH)_3$. The pit environment was acidic and bubbles of hydrogen rose from the surface forming corrosion chimneys. The hydrogen bubbles pump up $AlCl_3(OH)_3$ to the outside which reacts with water to form $Al(OH)_3$ (Burleigh et al., 1995). The pitting depth in temper T4 were lower than pitting depths in F and O tempers. It was reported that a high concentration of intermetallic compounds was observed at Al/SiC inter-phases which lead to localized corrosion (A). The corrosion rate of Al6013-20SiC (p) decreased for all tempers on increasing the temperature form 50 to 75°C and increased again on raising the temperature to 100°C. This change may be attributed to the changes brought about by the composition of the protective films from being bayerite (AlO(OH)) to boehmite (Al_2O_3, H_2) as shown by FTIR (Fourier transformation infra-red) spectroscopy).

The corrosion behavior of Al6013–20SiC (p) is a very strong function of Al (OH)3 and once the film formation is completed it becomes independent of oxygen (Beccario et al., 1994).
The crystals of boehmite have been observed on the surface of the alloy. The data generated in highly aggressive environment shows promising applications potential of this alloy in salt water and humid environment typical of sea coastal environment in the Gulf Region.

3.4 Effect of Inhibitors

It has been shown in earlier sections that Al/SiC metal matrix composites such as Al 6013-20 SiC (p) exhibit improved mechanical and physical properties compared to wrought alloys. However, they are more susceptible to pitting than their monolithic counterparts (Beccario et al., 1994; Trazaskama, 1990). They also exhibit a higher corrosion rate at velocities greater than the 2.3 ms^{-1} (Zaki, 2000). A variety of surface modification techniques such as anodizing, chromate conversion coatings and organic finishing have been suggested for the protection of aluminum metal matrix composite from localized corrosion (Aylor & Moran, 1986; Lin et al., 1989; Mansfield et al., 1990). Cerium coatings have been the focus of attention in the last decade (Hinton & Arnold, 1986; Davenport et al., 1991).
Studies on to investigate the effect of inhibitors on Al 6013 – 20 SiC (p) included weight loss, Electrochemical and re-circulation loop studies (Zaki, 2009).
Following inhibits solutions were used

a. 1000 ppm $K_2Cr_2O_7$ + 1000 pm $NaHCO_3$ + 3.5 wt % NaCl
b. 1000 ppm Cerium chloride + 3.5 wt% NaCl
c. 1000 ppm sodium molybdate + 3.5 wt % NaCl

The results of inhibitive action of $K_2Cr_2O_7$ + 1000 pm NaHCO3 are summarized in Table 10.

Alloy Designation	Velocity (ms-1)	Corrosion rate in mpy(MDD) with no inhibitor	Corrosion rate in mpy(MDD)with inhibitors
Al 6013-20 SiC(p)-O	1.0	11.8(22.1)	3.07(5.76)
	1.9	11.6(21.7)	7.63(14.32)
	2.7	12.9(24.1)	8.4(15.77)
	3.8	13.6(25.5)	9.63(18.08)
Al 6013-20 SiC(p)-F	1.0	9.9(18.5)	3.61(5.68)
	1.9	10.4(19.5)	4.31(8.09)
	2.7	10.8(20.2)	5.53(10.38)
	3.8	11.3(21.2)	6.60(12.39)
Al 6013-20 SiC(p)-T4	1.0	9.6(18.5)	2.01(3.77)
	1.9	10.1(18.2)	2.70(5.07)
	2.7	10.8(20.2)	3.40(6.38)
	3.8	11.4(21.4)	3.80(7.13)

Note; All experiments were conducted in 3.5 wt% NaCl

Table 10. The results of inhibitor action of k2Cr2O7+1000 ppm NaHCO3 (Zaki, 2009)

The reduction in the corrosion rate with $K_2Cr_2O_7$ +$NaHCO_3$ has been attributed to the formation of protective layer of boehmite Al $(OH)_3$, $3H_2O$ and bayrite Al_2O_3, H_2O. The breakdown of the oxide layer leads to pitting. The reduction in the corrosion resistance at increased velocities is caused by continuous removal of protective layer by erodent particles. The protrusion of particulates also makes it difficult to achieve a passivating layer; hence the resistance to the impact of velocity is lowered.

The preferred site for localized corrosion is Al/SiC interface as this site is abundant in intermetallic compound (Zaki, 1998). The existence of thermal stresses and dislocation density at interface affects the kinetics of erosion corrosion and increases the sensitivity if Al/SiC interfaces to erosion-corrosion. Because of the encouraging results of inhibition treatment of Al7057, and Al1000, with cerium chloride and sodium molybdate, studies were further conducted on Al6013 –20 Vol. % SiC(p) MMC. The effect of inhibition treatment is shown in Table 11 below.

		Corrosion rate in 3.5% NaCl+1000 ppm		Corrosion rate in 3.5% NaCl+1000 ppm Namoo4, CeCl3
Sr. No	Temperature °C	Temper	Mpy(mdd)	Mpy(mdd)
1	50	0	4.72(8.86)	3.8(7.13)
		F	2.24(4.13)	1.8(3.38)
		T4	1.71(3.21)	0.9(1.69)
2	70	0	8.3(15.5)	5.06(9.5)
		F	6.53(12.26)	4.01(7.5)
		T4	2.54(4.77)	2.01(3.72)
3	100	0	12.90(24.2)	8.05(15.11)
		F	11.60(21.7)	8.26(15.41)
		T4	10.19(19.13)	5.41(10.15)

Table 11. Effect of Inhabition Treatment

As shown by table 11 cerium chloride is a more effective inhibitor than sodium molybdate as shown by a larger reduction in corrosion rate brought about by addition of cerium chloride compared to sodium molybdate. The corrosion rate of temper of the MMC is reduced from 19.13 mpy to 3.96 with Cerium Chloride at 100°C which is very significant. Electrochemical studies were also conducted at 50, 70 and 100°C to observe the effect of temperature on inhibition. The electrochemical data obtained by above studies is shown Table 12.

The results of studies summarized in Table 12 clearly established that cerium chloride is a more affective inhibitor than sodium molybdate. The large difference between the corrosion potential (E_{corr}) and the pitting potential (E_p) shows that the cerium chloride is a more affective inhibitor in 3.5 wt % NaCl. The corrosion potential (E_{corr}) shifts closer to E_p which shows the sensitivity of the MMCS to localized pitting in Sodium Chloride without inhibition. The cathodic polarization curve of temper T4 of the alloy in 3.5 wt% NaCl +1000 ppm $CeCl_3$ in dearated condition is shown Figure 11. The curves are overlaid on the main curve. A maximum reduction in current density (from 234 to 25.1uA/cm2) is exhibited by Temper T4 in cerium chloride (Zaki, 2009). The current densities recorded are summarized in the Table 13.

Solution	Temperature °C	Temper	R(K.ohms)	E_{corr}(mv)	I_{corr}(µA/cm²)	Corrosion rate mpy(mdd)
Cerium Chloride	50	O	9.004	-0.8	3.727	1.60(2.99)
	50	F	3.301	-0.783	0.57	2.80(5.28)
	50	T.4	2.43	-0.78	1.1	0.47(0.88)
Cerium Chloride	70	O	1.281	-0.909	4.757	2.04(3.81)
	70	F	9.14	-0.915	3.993	1.68(3.14)
	70	T.4	10.07	-0.993	2.155	0.92(1.71)
Sodium Molybdate	50	O	44.5	-0.8	150	1.24(3.22)
	50	F	11.91	-0.716	216.5	1.92(3.60)
	50	T.4	41.3	-0.791	72.8	0.47(0.88)
	70	O	58.77	-0.909	272.6	2.74(5.11)
	70	F	23.76	-0.916	137.0	2.12(4.06)
	70	T.4	34.87	-0.867	111.5	0.75(1.46)
Sodium Molybdate	100	O	100	-0.87	100	8.60(16.00)
	100	F	100	-0.868	100	6.50(12.16)
	100	T.4	58	-0.947	74	3.96(7.41)

Table 12.

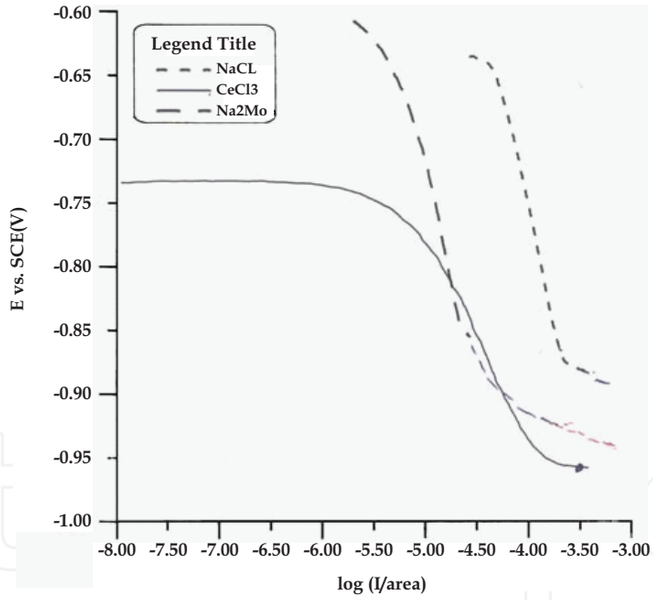

Fig. 11. A cathodic polarization curve of temper T4 of the alloy in 3.5 wt% NaCl + 1000 ppm $CeCl_3$ in deaerated condition (Zaki, 2009)

Sr. No.	Media	Icorr(µA | cm2)
1	3.5 wt % NaCl	234
2	3.5 wt% NaCl +1000 ppm Cecl3	25.1
3	3.5 wt% NaCl + 1000 ppm NaMoo4	178

Table 13. Current Densities of MMCS after Inhibition (Zaki, 2009)

Cerium chloride acts as a strong cathodic inhibitor for the alloy. Sodium molybdate on the other hand acts as an anodic inhibitor which acts by raising the pitting potential (Up) in the positive direction while maintaining E_{corr} negative to E_p. A typical cyclic polarization curve of the temper T4 of the alloy in 3.5 wt% NaCl + 1000 ppm $NaMoO_4$ is shown in Figure12. The corrosion potential tends to shifts to more positive values.

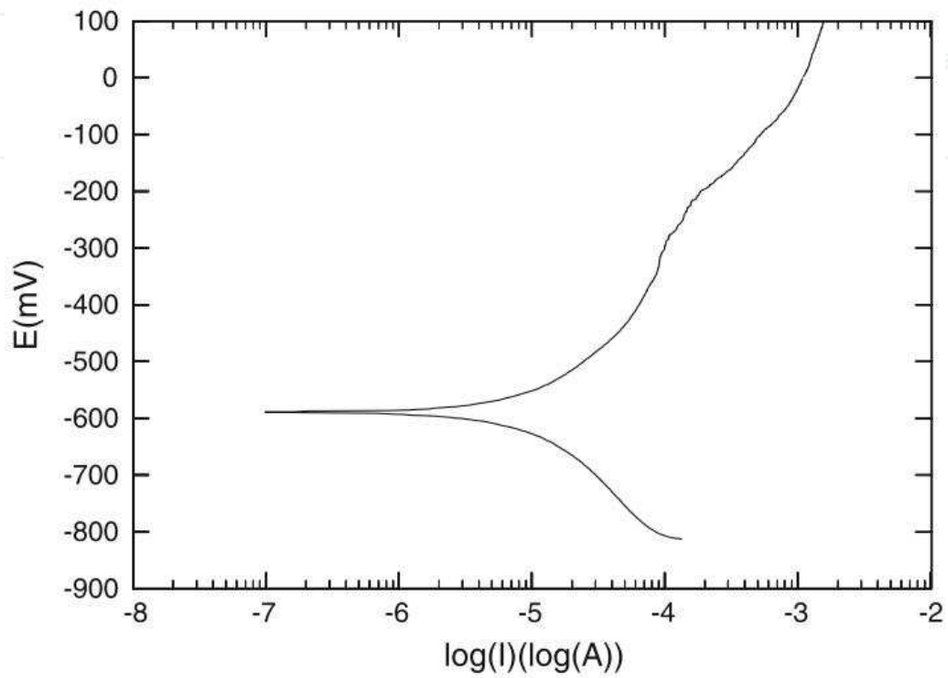

Fig. 12. A typical cyclic polarization curve of Al 6013-20 SiC (p)-T4 temper of the alloy in 3.5 wt.% NaCl + 1000 ppm sodium molybdate in deaerated conditions

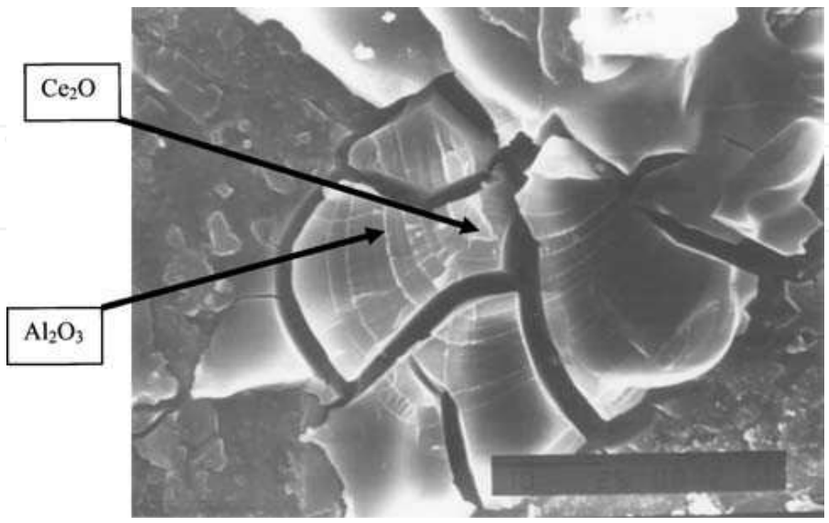

Fig. 13. Surface morphology of Al 6013-SiC (p) in 3.5 wt. % NaCl containing 1000 ppm CeCl3 (Zaki, 2009)

It is interesting to relate the surface morphology to localized corrosion. Typical features of surface morphology after inhibitor treatment are shown in figure 13. Deposition of two types of the particles in concentric rings is seen. These are particles of Ce_2O_3 and Al_2O_3. The square shaped particles of cerium oxide are shown in Figure 14. The oxide layer comprising of Ce_2O_3 and Al_2O_3 are very stable and protect the MMC from corrosion in 3.5 wt% NaCl. However, once the layer reaches a certain thickness, it flakes off. The broken oxide layer in

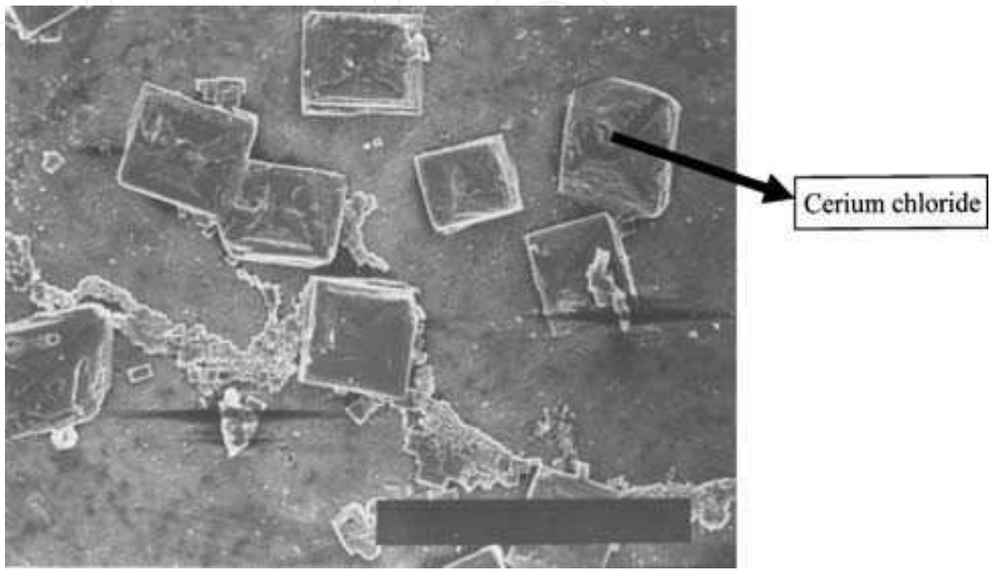

Fig. 14. Square-shaped particles containing predominantly cerium chloride formed on cathodic polarization (Zaki, 2009)

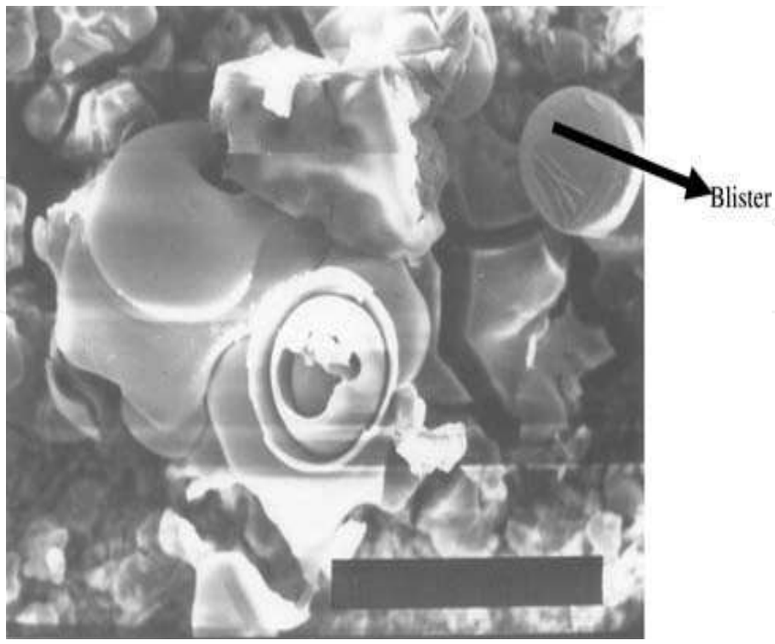

Fig. 15. Broken oxide layer forming blisters (mothballs)

the form of mothballs can be observed in Figure 15. It has been reported that cathodic reaction proceeds at the sites of intermetallic precipitates of copper and its solution becomes alkaline. The film of cerium oxide replaces the film of aluminum hydroxide with increased exposure time (Muhammad & Edwin, 2004; Misra et al., 2007). Whereas the studies on the inhibition of AlMMC are still lacking, there is sufficient evidence to show that cerium chloride is an effective inhibitor for corrosion protection of AlMMC Sodium molybdate is not as effective as cerium chloride shown by the studies reported above composite in chloride containing environment.

3.5 Corrosion mechanism

Despite decades of research no conclusive mechanism on the localized corrosion of Al/SiC(p) composites has been described – The role of intermetallic and dislocation generation at Al/Sic (p) interface has not been conclusively established. No attack a SiC particles has been reported in literature.

From several reliable studies it may be concluded that the pitting potential of monolithic alloys depends on the alloy composition and Ep which is more positive than that of reinforced material (Monticelli et al., 1997; Trazaskoma et al., 1990). The pitting resistance of several MMC investigated followed the order, Al2024 = Al6013 – 20Sic (p) > AL 6061>, Al 6013-20SiC (p) T4=Al5456 (Zaki 2000). In the studies conducted an abundant distribution of copper and secondary phase particles of Mg and Fe were observed.

Copper particles were also present in pit cavities. Analysis of corroded regions at the interface showed a greater concentration of copper compared to the surface away from the interface. The presence of $AlCl_3$ in the oxide film has been indicated by EDS studies (Trazaskoma et al., 1990). Results show a high concentration of copper (3.5%) and Fe (1.77%). There is therefore, a sufficient evidence to show that the increased reactivity at the interface is responsible for localized corrosion of composites. The intermetallic precipitates act as anodic or cathodic sites for initiation of localized corrosion. It is also observed that homogenization of the surface minimizes corrosion the reactivity at the interface is further minimized as shown by temper T4. The SiC particles do not provide any sites for initiation of pits. A higher concentration of copper in pit cavities may be attributed to higher velocities which transport copper ions. Dislocation generation at the interface further activates the interface.

Two more factors are reported to influence, the mechanism of corrosion; Na:YAG laser treatment and machining. Electrochemical studies undertaken showed that the corrosion potential (E_{corr}) increased by 79mv and the corrosion current density decreased by an order of magnitude for the laser treated specimens whereas the untreated surface showed extensive corrosion accompanied by abundant pits. The decrease of corrosion is reported to be due to reduction in the concentration of intermetallic precipitates.

The effect different machining conditions, WEDM, Carbide Turning and Diamond Turning on the electrochemical corrosion behaviour are shown in Figure 16. No significant difference in pitting corrosion potential between the three machining condition was observed. The magnitude of corrosion current for the three machining conditions however differed. Diamond turned specimens showed shallow pits at isolated sites accompanied by a high corrosion rate, whereas Carbide Turned specimens showed extensive pitting because of the hindrance of repassivation of pits due to micro and large crevices present on the surface, pits developed were deeper.

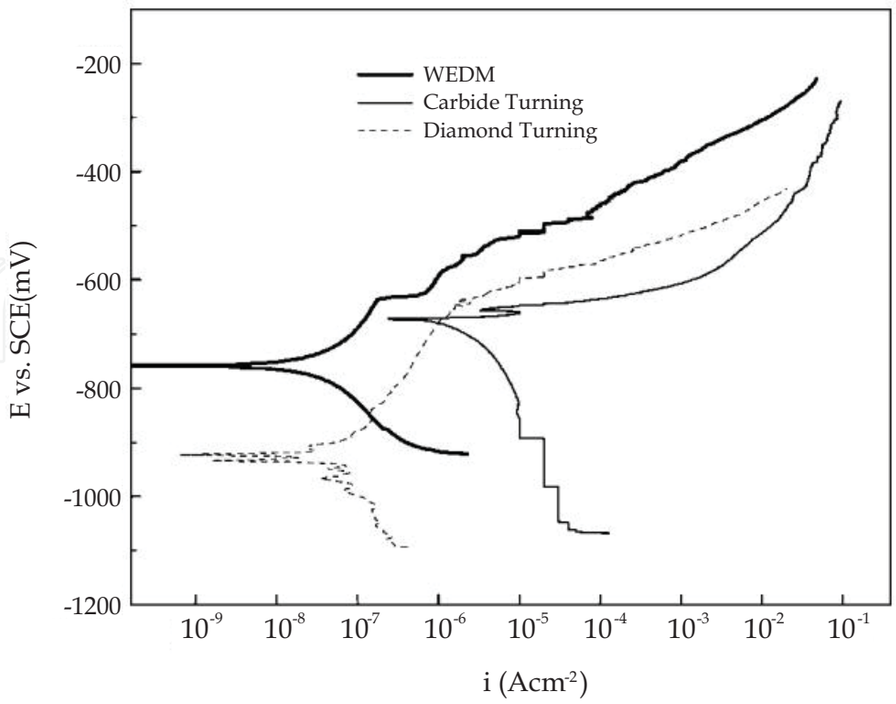

Fig. 16. Potentiodynamic polarization curves of the composite machined to different conditions (Yue et al., 2002)

In the eclectically discharged machined specimen, a resolidified layer of aluminium provided a blanketing effect on the substrate. A reasonable range of passivity was produces on the surface. The high resistance was provided by a layer of oxide on the resolidified aluminium layer created by machining. From the above evidence it is to be understood that surface morphology plays an important role at the Al /SiC interface. Scanning micro reference studies has been employed for direct mapping the active centers on surface of electrode with a low dimensional resolution in micrometers. Evidence of micro pitting has been observed at the open-circuit potentials which were more negative than the pitting potential. In their studies, the same conclusion was reached; i. e the SiC/Al interface is the active center for localized corrosion due to the precipitation of intermetallic compounds (Zaki, 2000).

The observation that heat treatment increases corrosion resistance is shown by temper T4 of Al6013 /20 SiC (p), it is further supported by studies on temper T6 of Al2009/SiC (w), which showed a higher resistance to pitting compared to as rolled specimens It has been already stated above their heat treatment induces homogenization which causes a reduction in the concentration of intermetallic compounds and hence, reduces localized Corrosion.

From the above discussion it may be concluded that the composites are more sensitive to pitting than their monolithic counterparts unless they are subjected to T4 or T6 heat treatment. These is sufficient evidence to show AL/SiC interface is the main target of localized corrosion due to the presence of intermetallic particulates and inclusion which may form micro-galvanic cells and induce localized corrosion. It is also observed that SiC particles are not attacked.

Surface treatment has a significant effect are localized corrosion as shown by the effect of laser treatment and effect of machining on the surface. The scanning micro effloresce electrode studies have shown that Sic/Al interface is the centre f localized corrosion.
Although no conclusion mechanism of localized corrosion of Al MMC exists, there is sufficient evidence to show that Al/SiC interface acts as a centre for localized corrosion and a reduction in the concentration of intermetallic compounds is accompanied by a reduction in localized corrosion as shown by the effect of tempers T4 and T6 on localized corrosion.

4. Conclusion

Based on the studies conducted in the last they decades, the following are the major conclusion on the mechanical and corrosion behaviour of Al MMCs

1. The mechanical properties of fiber, particulate, or whisker reinforced composites are strongly dependent upon the micro-structural parameters, size, shape, orientation and volume fraction of the reinforcement.
2. The tensile strength and Vickers micro-hardness increases significantly with increasing volume fraction of reinforcement as exemplified by Al6013, 6061, 2024 reinforced with particulate and whiskers. The strain to failure also decrease with increased volume fractions of reinforcement - Sliding velocity leads to lower wear rates and lower frication coefficient as shown by SiC and B_4C reinforcements.
3. Increasing cutting speed increased tool wear. The highest wear rate was shown by 15 wt% SiC (p) and the lowest by 5 wt% SiC.
4. Because of accumulation of stress concentration and high dislocation density Al MMC's are sensitive to stress corrosion cracking is 3.5 wt% NaCl – Al6061/20vol% SiC(p)-T6 shows a good resistance to stress corrosion cracking. The polarization curves shifted to higher current densities.
5. The corrosion rates of MMC's decreased with exposure time in long term immersion tests. Heat treatment lowered corrosion rates because of the homogeneous distribution of the precipitates an reduction in their concentration on the Al/SiC interphase electrochemical studies on MMC's showed that the pitting potential decreased with increasing volume fraction of SiC(p) in Al6013 and 6061 reinforce with SiC particulate. Shallow pits contain intermetallic $CuAl_2$.
6. The effect of machining conditions on corrosion showed that electrical discharge machining provided higher resistance to pitting than carbide turning or diamond turning machining.
7. The lowest rate of corrosion was shown by temper T4 if A6013 – 20 SiC(p) is 3.5 wt% NaCl containing silica and other particulate matter.
8. Studies in salt spray chamber showed a good resistance of MMC's to Corrosion and Heat treatment enhances corrosion resistance in corrosive environment.
9. MMC's exhibited a beneficial effect of inhibitor treatment with cerium chloride and sodium molybdate. Cerium Chloride has paved away more effective inhibition than sodium molybdate.
10. The mechanism of corrosion of MMC's is not conclusively understood. It has been, however, shown that the Al/SiC interface us highly reactive due to the presence of intermetallic compounds.

5. References

ASTM; Recommended Practice Designation G 31.72, Standard Practice for Laboratory immersion Testing, (2004) Vol 03, ASTM, Ohio, USA.

Aylor D. M, Moran P. I, Effect of Reinforcement on the pitting Behavior of Aluminum Based Metal Matrix Composites, Jr Electrochem Soc, (1986), Vol 30, p951.

Beccario A.M, Paggi G, Cingaud D, Castellor P, Silicon Carbide Alloy Metal Matrix Composites , Br Jr Corrosion, (1994), Vol 29(1), p65.

Beccario A. M, Poggi G. J, Ginguad D, Castello, Effect of Hydrostatic Pressure on Passivating Powder of Corrosion Layers Formed on 6061-T6 Aluminum Alloy in Sea, Br. Corros Jr, (1994), Vol 29, 1, pp 65-69.

Berkely, D.W, Sallam H.E, Nayeb. Hasemi, H,; The effect of PH on the mechanism of Corrosion and Stress Corrosion and Degradation of Mechanical Properties of AA 6061 and Nextel 440 Fiber-Reinforced AA 6061Composites, Corros Sc,(1998), Vol 40, 2/3 pp, 141-153.

Burleigh T.D, Ludwiczak and Petro R.A, Itergranular Corrosion of an Aluminum Magnesium Silicon Copper Alloy, Corrosion Science, (1995), Vol 5199(1), p50.

Chen C, and Mansfeild F, Corrosion Protection of Al 6092/SiC (p) Metal Matrix Composite, Corr Sc, (1997),Vol 6, PP 1075-108.

Colman S. L, Scott V. D, Enaney M.C, Corrosion Behavior of Aluminum Based Metals Matrix Composites, (2011), Vol 297, 11, Dol: 10.10078/BF001117589, Jr of Mat Sc.

Davenport A. J, Isacs H. S, Kendig M. W; Investigations on the Role of Cerium Compound on the Corrosion Inhibition of Aluminum, Corrs Sc,(1991),Vol 32 (516), p653.

Dehlan Al Khalid; Hafeez Syed, Tensile Failure Mechanism of Al 6061Reinforced with Submicron Al2O3, AJSE, (2006), Vol 31, No 2C.

Feng.Z; Lin, C; LinJ; Lin j; Luo, J; "Pitting Behavior of SiC/2024 Al MMC".

Griffen, A.J; Turnbull, A; 'An Investigation on the Electrochemical Polarization Behavior of Al6061 MMC' Corros Sc (1994), Vol 36,1, 21-35.

Hihara L. H, Corrosion of Metal Matrix Composites, Shriers Corrosion, (2010), Vol 3, pp 2250-2569.

Hinton B. R. W, Dr. Arnold Ryan N. E; Cerium Conversion Coating for Corrosion Protection of Aluminum, Mat. Forum, (1986), Vol 9(3), pp 162.

Hongho Ding, Hawthorn, G.A, Hihara, L.H, Inhibative Effect of Sea Water on the Corrosion of Particulate Reinforce Aluminium Matrix Composites and Monolithic Alloys, Jr. Electrochem Soc, (2009) 156, (100. (35).C159.

Isacs, H.S, Vyas, B; "Electrochemical corrosion Testing, ASTM, STP 727, 1981, p, 3.

Jamaludin, S.B, Yusoff Z, Ahmed R.R, Comparative Study of Corrosion Behavior of A.A. 2009/20 Vol% SiC(w), Porpugaliay Electrochimica Acta, (2008), Vol 26, pp 291-301.

Lin, S; Shih, H; Mansfield F; Corrosion Protection of Aluminium Alloys and Metal Matrix Composites by Polymer Coatings; Corros Sc (1992), Vol 23, 9, pp 1331-1349.

Lin S, Greene H. Shih and Mansfeld F, Corrosion Protection of Al Metal Matrix Composites, Corrosion, (1989), Vol 45(8), p615.

Mansfield S, Lin S, Kim H, Shih, Pitting and Passivation of Al Based Metal Matrix Composites, J Electrochem Soc, (1990), Vol. 137, pp 75-82.

Mansfield F. S.L. Jeanjagnet; The Evaluation of Corrosion Protection Measures For Metal Matrix Composites, Corros Sc (1984), Vol 26, pp 727-734.

Misra, Ajit Kumar, Balsubramanium, Corrosion Inhibition, Material Chemistry and Physics, (2007), Vol 103, 2, 3, pp 385-393.

Monticelli C, Zucchi C, Bruuonoro, Trabanelli C, Stress Corrosion Cracking Behaviour of some Aluminum Base Metal Matrix Composites, Corrs Sc, (1997), Vol 39,10, pp. 1949-1063.

Muhammad Ashraf, P. Leela Edwin, Evaluation of Corrosion Inhibition by Cerium on Aluminum under Marine and Laboratory Environment, 2nd Jr of Chem. Tech, (2004), Vol 11, pp 672-677.

Rohatgi, P.K; 'Aqueous corrosion of Metal Matrix Composites, Comprehensive Composite Materials, (2003), Chapter 3.18, , pp 481-500, Elsevier

Schwartz, M.M "Composite Material Processing Fabrication and Applications" Prentice Hall, USA (1997).

Shorowords,K.M; Haseeb, A.S.M.A; Celic,j.P; "Studies on the wear Friction and Tribochemistry of MMC Sliding against Phenolic Brake Pads, Wear" (2004), pp1176-1181

Turnbull, A.Br, Corros Jr 1992, Vol 27, p.27-35.

Trzskoma, P.P; in "Metal Matrix Composite Mechanism and Properties" Academic Press, (1991), p, 383.

Trazaskama P. P, Pit Morphology of Aluminum Alloy in Silicon Carbide Alloy Metal Matrix Composites, Jr Corrosion, (1990), Vol 46, p402.

Trazaskoma P.P, Maccefferty E, Crowe C.R, Corrosion Resistance of Al Based Metal Matrix Composites, Corrs Sc, (1990), 46, p402.

Vaeeresh Kumar, G.B., Rao, C.P; Selvararj.N; Bhagya Shekar, M.S.B; Studies on Al 6061-SiC and Al 7075-Al2O3 Metal Matrix Composite; Jr for Mater and Mater characterization and Eng, Nov (2010), Vol 9, pp, 43-55.

Vogelsang, M; Arsenault, R.J; Fisher, R.M; In SituHVEM study of Dislocation Generation of Al/SiC Interface in Metal Matrix Composites, Met.Trans A, (1986), Vol 17A, p139.

Yue, T.M; Yu, J.K; Maki, H.G; "Corrosion Behavior of Aluminium 2009/SiC Composite Machined to Different Conditions". Jr Mat Sc Letters, (2002), Vol 21, 14, pp1069-1072

Yue, T.M; Wu, Y.X; Man, H.c; 'On the Role of CuAl2 Precipitates in Pitting Corrosion of Aluminium (2009), SiC Metal Matrix Composites' Jr of Materials Sc (2000), Letters 9, pp 1003-1006.

Zaki Ahmad and Abdul Aleem B. J, The Effect of Inhibitors on the Susceptibility of AL 6013, SiC Interface to Localized Corrosion, Jr of Mat Eng, Perf,(2009),Vol 18,2, pp129-136.

Zaki Ahmad, Mechanical Beauvoir and the Fabrication Characteristics of Aluminum Metal Matrix Composites, Jr of Reinforced Composite Material, (2007),Vol 1, 4, pp 3027-3033.

Zaki Ahmad, Abdul Aleem. B.J; Degradation of Aluminium Metal Matrix Composites in Salt Water and its Control, Mater and Design, (2001), Vol 23, pp173-180.

Zaki Ahmad, Paulette, P.T; and Aleem B.J.A; "Mechanism of Localised Corrosion of Aluminium Silicon Carbide Composites in a Chloride Containing Environment' Jr. Mat Sc (2000), 35, pp 2573-2579.

Zaki Ahmad & Abdul Aleem B. J, Corrosion Resistance of a New Al 6013-20 SiC in Salt Spray Chamber, Jr of Mat SC and Eng, (2000), Vol 9, 3l, p338.

Zaki Ahmed & Abdul Aleem B.J, Corrosion Resistance of New Aluminium Al 6013/20SiC(p) in Salt Spray Chamber,Jr Mat Sc and Eng,(2000),Vol 9(3),p338.

Zaki Ahmed, Paulette, P, T, Aleem B.J.A, Mechanism of Localize Corrosion of Aluminum Silicon Carbide Composites in Chloride Containing Environment, Jr Mater Sc,(2000),Vol 3, 5, pp2573-2579.

Zaki Ahmad & Abdul Aleem B. J, The Erosion Corrosion of Al -SiC Composites in Sea Water, (1998), Final Report, KACST, 14-65, King Abdul Aziz City of Science and Technology, Riyadh, Saudi Arabia.

Lima, P.; Bonarini, A. & Mataric, M. (2004). *Application of Machine Learning,* InTech, ISBN 978-953-7619-34-3, Vienna, Austria

Li, B.; Xu, Y. & Choi, J. (1996). Applying Machine Learning Techniques, *Proceedings of ASME 2010 4th International Conference on Energy Sustainability*, pp. 14-17, ISBN 842-6508-23-3, Phoenix, Arizona, USA, May 17-22, 2010

Siegwart, R. (2001). Indirect Manipulation of a Sphere on a Flat Disk Using Force Information. *International Journal of Advanced Robotic Systems,* Vol.6, No.4, (December 2009), pp. 12-16, ISSN 1729-8806

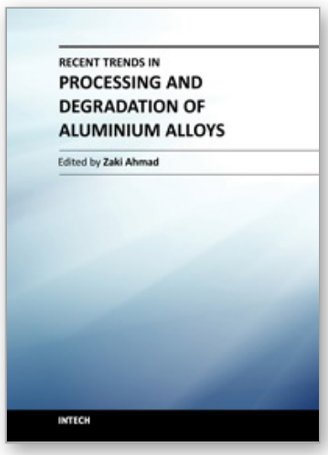

Recent Trends in Processing and Degradation of Aluminium Alloys
Edited by Prof. Zaki Ahmad

ISBN 978-953-307-734-5
Hard cover, 516 pages
Publisher InTech
Published online 21, November, 2011
Published in print edition November, 2011

In the recent decade a quantum leap has been made in production of aluminum alloys and new techniques of casting, forming, welding and surface modification have been evolved to improve the structural integrity of aluminum alloys. This book covers the essential need for the industrial and academic communities for update information. It would also be useful for entrepreneurs technocrats and all those interested in the production and the application of aluminum alloys and strategic structures. It would also help the instructors at senior and graduate level to support their text.

How to reference
In order to correctly reference this scholarly work, feel free to copy and paste the following:

Zaki Ahmad, Amir Farzaneh and B. J. Abdul Aleem (2011). Corrosion Behavior of Aluminium Metal Matrix Composite, Recent Trends in Processing and Degradation of Aluminium Alloys, Prof. Zaki Ahmad (Ed.), ISBN: 978-953-307-734-5, InTech, Available from: http://www.intechopen.com/books/recent-trends-in-processing-and-degradation-of-aluminium-alloys/corrosion-behavior-of-aluminium-metal-matrix-composite

INTECH
open science | open minds

InTech Europe
University Campus STeP Ri
Slavka Krautzeka 83/A
51000 Rijeka, Croatia
Phone: +385 (51) 770 447
Fax: +385 (51) 686 166
www.intechopen.com

InTech China
Unit 405, Office Block, Hotel Equatorial Shanghai
No.65, Yan An Road (West), Shanghai, 200040, China
中国上海市延安西路65号上海国际贵都大饭店办公楼405单元
Phone: +86-21-62489820
Fax: +86-21-62489821

IntechOpen